Digest Journal of Nanomaterials and Biostructures Vol. 9, No. 1, January - March 2014, p. 423 - 431

VARIATIONS OF OPTICAL AND STRUCTURAL PROPERTIES WITH TEMPERATURE FOR Cr_xO_y THIN FILMS SYNTHESIZED IN A POLYMER MATRIX BY CHEMICAL BATH DEPOSITION TECHNIQUE

A.B.C EKWEALOR*
Department of Physics and Astronomy, University of Nigeria, Nsukka

The effects of temperature on the optical and structural properties of chromium oxide thin films synthesized in the pores of PVP by chemical bath deposition technique were investigated. Films deposited with varying temperature were crystalline. The optical properties of the films were derived from absorbance, transmittance reflectance, refractive index, absorption coefficient and extinction coefficient measurements. The synthesized Cr_xO_y films which were dark grayish yellow-green in colour, were observed to be Eskolaite, Cr_2O_3 nanocrystals of size 16.47nm; however, as annealing temperature was increased, the size increased to 27.96nm. The absorption coefficient, refractive index and extinction coefficient were found to decrease with increase in annealing temperature. For the same energy ranges of the incident photons, the ranges of absorption coefficient and refractive index were 0.2 – 1.7 and 1.50 – 2.40 respectively. The energy band-gap of the films ranged from 2.10eV to 2.70eV.

(Received January 24, 2014; Accepted March 27, 2014)

Keywords: Chromium oxide, Annealing temperature, CBD, Band gap and optical properties

1. Introduction

Chromium oxide, Cr_2O_3 consists of the rhombohedral primitive cell, where Cr atoms are eight-coordinated with two oxygen layers. They form CrO_6 distorted octahedra that are linked by faces, edges or corners in such a way that each oxygen atom is linked to four Cr atoms [1]. Many crystalline modifications of Cr oxide exist, such as Cr_2O_3 (corundum), CrO_2 (rutile), Cr_5O_{12} (three-dimensional framework), Cr_2O_5 and CrO_3 (unconnected strings of CrO_4 tetrahedra). The only stable bulk oxide, Cr_2O_3, is a magnetic dielectric with corundum structure [2].

Among the various chromium oxides, Cr_2O_3 is the most stable under ambient conditions [3]. Cr_2O_3 materials find applications in protective coating layer [4], solar absorber for thermal collectors [5], various catalytic systems [6], NO_x gas sensor [7], anode material for Li-ion batteries [8], and material for solid oxide fuel cell [9]. Cr_2O_3 thin films have also been widely used as protective coatings against wear, corrosion and oxidation [10]. Optical applications of Cr_2O_3 thin films include electrochromic coatings [11], infrared (IR)-transmitting coatings [12], selective black absorbers [13], and optically selective surfaces of solar collectors [14]. Low-reflective Cr_2O_3/Cr films are also widely used as black matrix films in liquid crystal displays [15].

A wide variety of chemical and physical methods have been used for large area synthesis of Cr_2O_3 films, e.g. chemical vapour deposition (CVD) at either atmospheric [16] or low pressure [17], plasma enhanced CVD (PECVD) [18], electrodeposition [19], metal oxidation [20], chemical spray pyrolysis [21], RF magnetron sputtering [22], molecular beam epitaxy [23] and atomic layer deposition [24]. However, very little had been reported on production of these films in polymer matrix by CBD method. Here, a report on the effect of annealing temperature on the optical and structural properties of chromium oxide thin films obtained by chemical bath deposition techniques is presented.

* Corresponding author: abcekwealor@yahoo.com

2. Experimental details

2.1 Synthesis of Chromium Oxide Cr_xO_y Films

Glass substrates were first degreased in a mixture of concentrated HCl and HNO_2 for about 30 hours. They were then washed clean in a cold powder detergent solution, rinsed in distilled water and dried in an oven. Other apparatuses used for the experimental work were also thoroughly washed with detergent and rinsed with distilled water. Polyvinylpyrrolidon (PVP) solution, prepared by dissolving 4 grams of solid PVP in 400 cm^3 of distilled water, was stirred in a magnetic stirrer for about one hour until a homogeneous solution was obtained. This constituted the polymer matrix.

The chemical bath for this experiment was prepared by mixing and stirring 5ml of 1M $CrCl_3$, 15ml of 1M Triethanolamine (TEA), 15ml of 13.4M NH_3 and 40ml of PVP in a 100 cm^3 beaker. The pH value of the solution was 9.8. TEA served as complexing agent. To ensure equal parameters of deposition, five substrates were immersed in the same bath and supported by the wall of the beaker. The bath temperature was kept at 343K and the substrates were left in the bath for three hours to allow for substantial deposition. The substrates were then removed, rinsed in distilled water and dried in an oven. They were later annealed at different temperatures.

2.2 Optical Characterization of Cr_xO_y Thin Films

The optical properties of the films were studied using absorption spectra in UV–VIS–NIR regions obtained from Unico UV – 2102 PC spectrophotometer at normal incidence of light within the wavelength range 200nm – 1200nm.

2.3 Results and Discussion

The deposited Cr_xO_y films had a dark grayish yellow-green colour and showed good adhesion to the glass substrates. Plots of absorbance, transmittance and reflectance against wavelengths for the Cr_xO_y films at varying concentrations are given by figs. 1 – 3 respectively. From fig. 1 which is a plot of absorbance against wavelength, it can be seen that all the films have high absorbance from 45% – 35% respectively in the UV-VIS region, but this decreased unto the NIR region to about 22% – 12% respectively. Here, absorbance is seen to decrease with increase in annealing temperature.

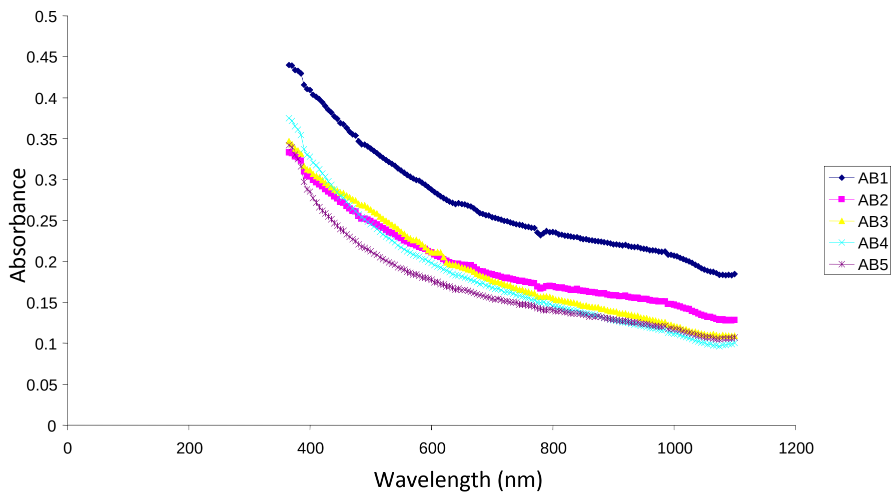

Fig 1: Absorption spectra for Cr_xO_y thin films with varying annealing temperature

All the films deposited have moderate transmittance between 31% – 45% in the UV-VIS region, but progressively increased to about 57% – 74% respectively in the NIR region. This can be seen from fig. 2 which gives the variation of transmittance against wavelength. The lower value of transmittance in the UV-VIS regions could be due to light scattering from rough surface and/or defect states [25]. It can also be seen that the transmittance of the films increased with annealing temperature; with the as deposited film showing the least transmittance. This implies that the films are more transparent in the VIS-NIR region. This correlates with report by other researchers [26]. The properties of poor transmittance in the UV-VIS, but moderately high transmittance in the VIS-NIR exhibited by as deposited film, make the film good material for screening off UV portion of electromagnetic spectrum which is dangerous to human health and as well harmful to domestic animals. The film can be used for coating eye glasses for protection from sunburn caused by UV radiations [27].

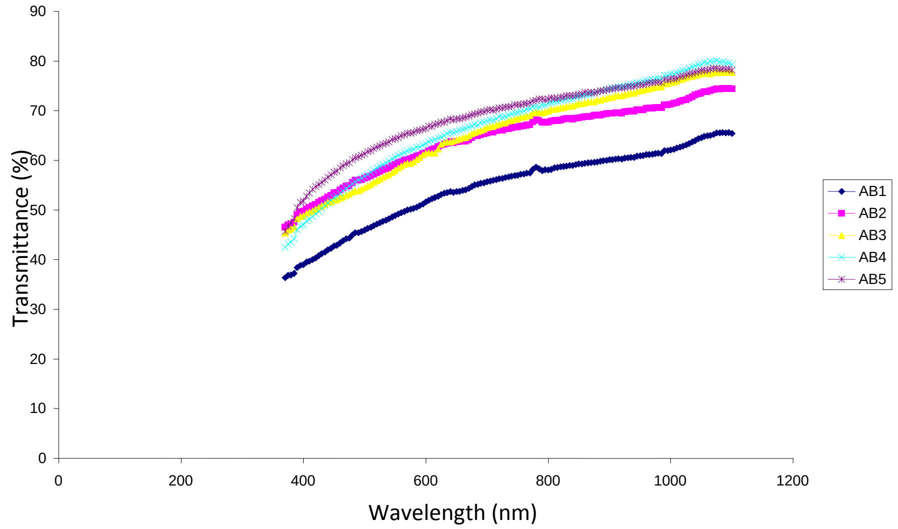

Fig 2: Transmittance spectra for Cr_xO_y thin films with varying annealing temperature

From fig. 3 which gives a plot of reflectance against wavelength, it can be observed that all the films showed moderate reflectance of about 20% in the UV-VIS region, but this decreased progressively to about 18% – 12% respectively in the NIR region. Again, the reflectance of the films decreased with increase in annealing temperature.

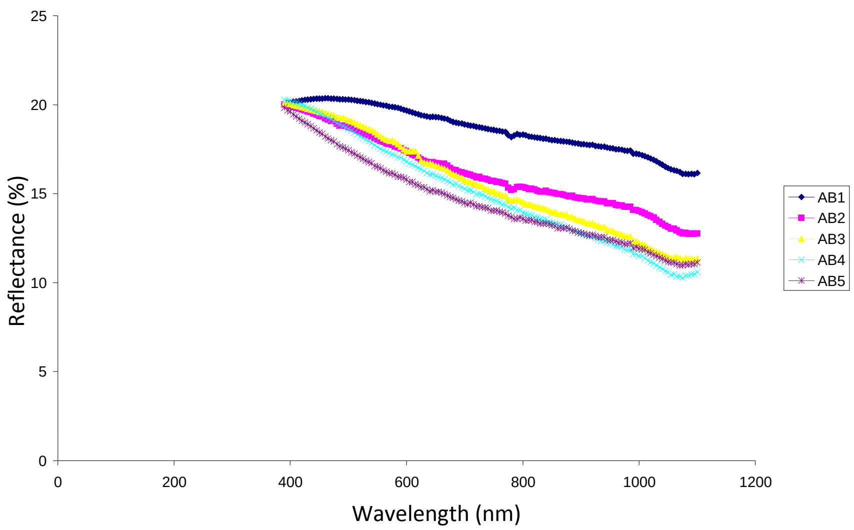

Fig 3: Reflectance spectra for Cr_xO_y thin films with varying annealing temperature

The equation derived for the determination of energy band gap values (Eg) is given as [28]

$$\alpha(hv) = \frac{A}{hv}(hv - E_g)^m \quad (1)$$

where m = ½ for allowed direct transition, m = 3/2 for direct ''forbidden'' transition, m = 2 for allowed indirect transition and m = 3 for indirect ''forbidden'' transition, A is a constant nearly independent on photon energy and known as the disorder parameter.

The energy band-gap of the Cr_2O_3 films increased with increase in annealing temperature as can be seen in the plot of band-gap against photon energy given by fig. 4. This can be attributed to better crystalline quality and oxygen deficiency after annealing; however, the effect of these processes is still not well known [29]. This relation agrees with report of Al-Kuhaili and Durrani [30]. The E_g values ranged from 2.10eV – 2.70eV. Annealing process has been noted to be helpful in improving the electro-optical properties of thin films [31].

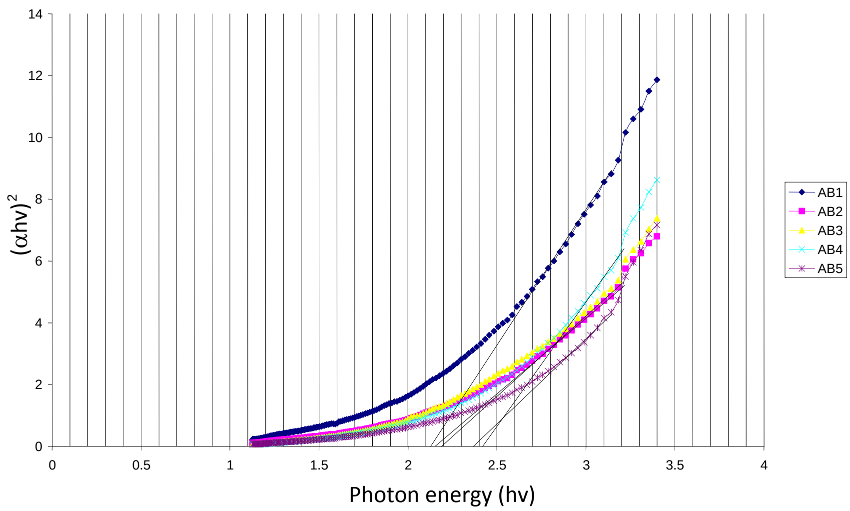

Fig 4: Band-gap spectra for Cr_xO_y thin films with varying annealing temperature

The absorption coefficient decreased with annealing temperature as shown by fig. 5 which is the absorption coefficient plot against photon energy of radiation; this relates favourably with the reports of Oboudi et al [32] and Al-Kuhaili op cit. It can also be observed that the absorption coefficient increased with increase in energy of radiation. For the energy range 1.0 – 4.0eV, the absorption coefficient ranged from 0.2 – 1.7.

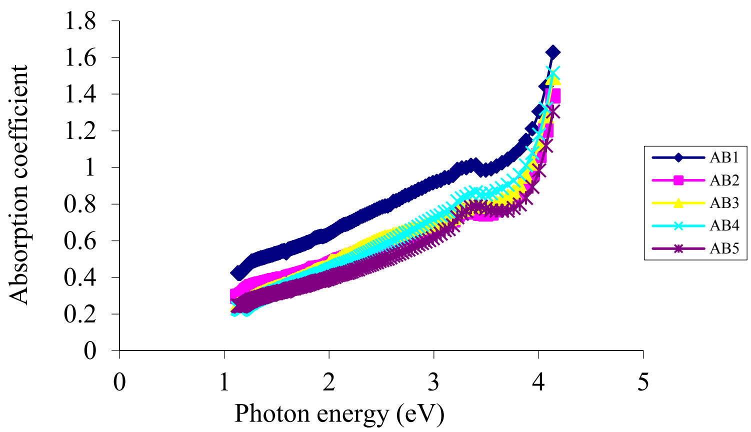

Fig 5: Absorption coefficient spectra for Cr_xO_y thin films with varying annealing temperature

Fig. 6 is a plot of refractive index, n, against photon energy for the Cr_xO_y thin films annealed at different temperatures. It shows that the refractive index of the films decreased with increase in annealing temperature; but increased with increase in photon energy of radiation this also agrees with the report of Oboudi et al, op cit. The refractive index values for these films range from 1.5 – 2.5.

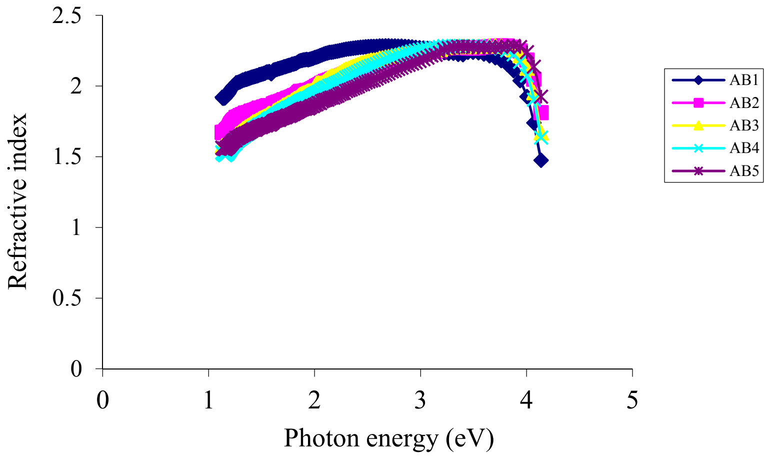

Fig 6: Refractive index spectra for Cr_xO_y thin films with varying annealing temperature

The extinction coefficient, *k*, and absorption coefficient, *α*, are related by equation (2) [33].

$$k = \frac{\alpha\lambda}{4\pi} \tag{2}$$

where *λ* is the wavelength of incident radiation. From fig. 7 which gives the plot of extinction coefficient against photon energy of radiation, the extinction coefficient is seen to decrease with annealing temperature. The values however, showed slight variation for the annealed films than those of the as deposited film. This indicates that when the films were annealed, their extinction coefficient did not vary much from the visible region to the NIR region.

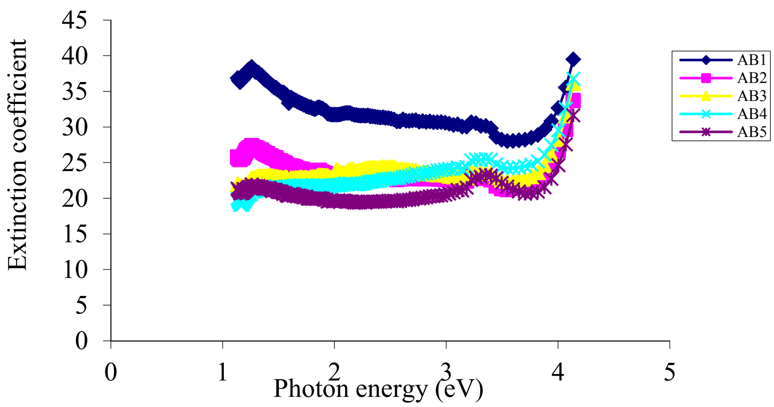

Fig 7: Extinction coefficient spectra for Cr_xO_y thin films with varying annealing temperature

The dielectric constant, ε, is related to the extinction coefficient, k, and the refractive index, n, by the equations (3) and (4) [34]

$$\varepsilon_r = n^2 - k^2 \qquad \text{(for real part)} \qquad (3)$$

and

$$\varepsilon_i = 2nk \qquad \text{(for imaginary part)} \qquad (4)$$

Plots of real and imaginary dielectric constants against photon energy are given by figs. 8 and 9. From these, it can be seen that both the real and imaginary dielectric constants decreased with increase in annealing temperature. However, whereas the value of ε_r increased with increase in photon energy

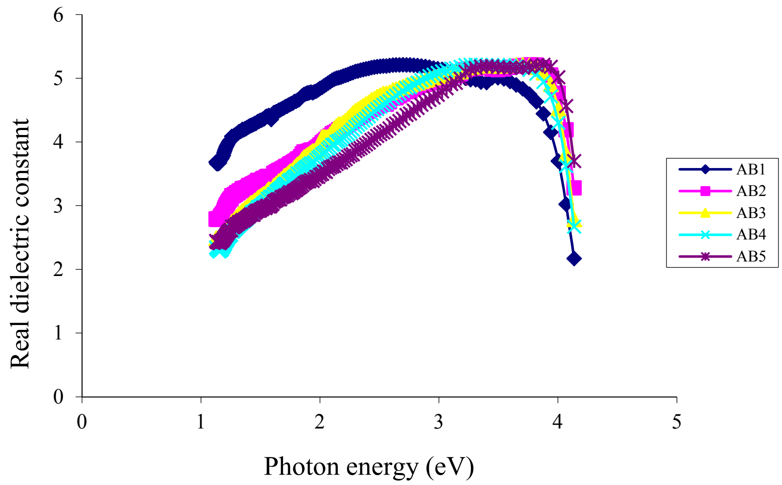

Fig 8: Real dielectric constant spectra for Cr_xO_y thin films with varying annealing temperature

for all the films, the value of ε_i increased only for annealed films, for the same energy range. The value of ε_i for the as deposited film rather decreased with increase in photon energy. Fig. 9 also shows that at about the highest photon energy, the value of the imaginary dielectric constant of annealed films was a maximum, while that for the as deposited was a minimum. This behaviour of the annealed films could be attributed to denser films, arising from evaporation of water molecules off the films [35].

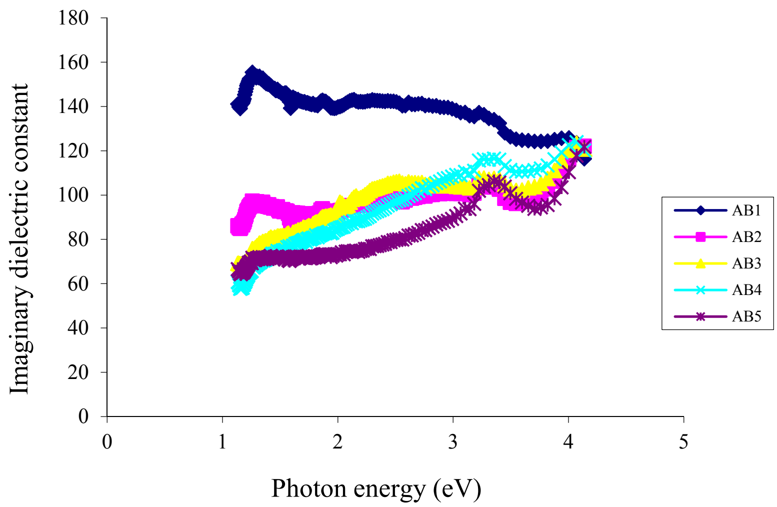

Fig 9: Imaginary dielectric constant spectra for Cr_xO_y thin films with varying annealing temperature

3. Structural Characterization of Cr_xO_y Thin Films

The structural characterization, was carried out by subjecting the films to X-ray diffraction (XRD), in the range of scanning angle 2θ with Cuk_α radiation (λ = 1.5406Å) using Philips P.W 1500 X-ray diffractometer.

3.1 Results and Discussion

The XRD spectra for the films with varying annealing temperatures given by figs. 10 – 12 show that the films were chromium oxide, Cr_2O_3; Eskolaite. Fig. 10 which is the spectra for the as deposited film, shows peak at 73.50°, which corresponds to diffraction line produced by (119) plane.

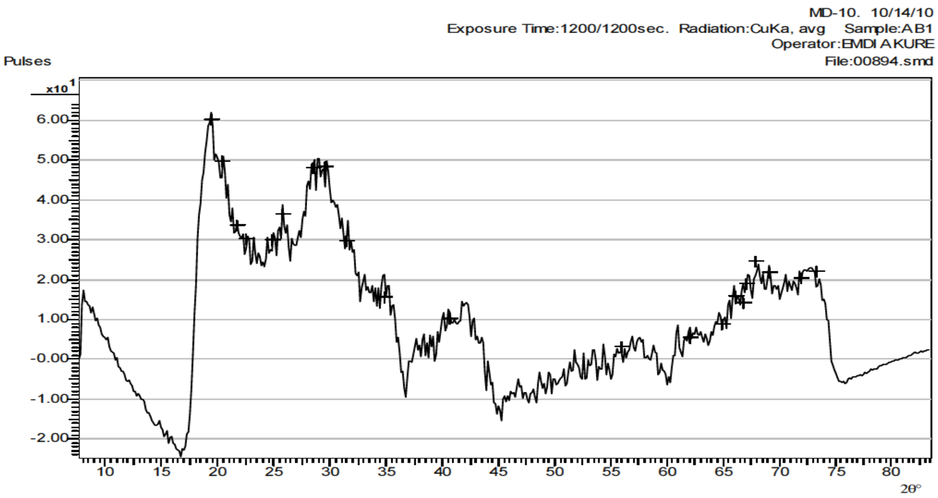

Fig 10: XRD diffractogram for as deposited Cr_2O_3 films

The film annealed at 473K given by fig. 11, shows peak at 2θ = 72.92°; corresponding to diffraction line produced by (1010) plane. This fairly agrees with result obtained by Wang et al [36].

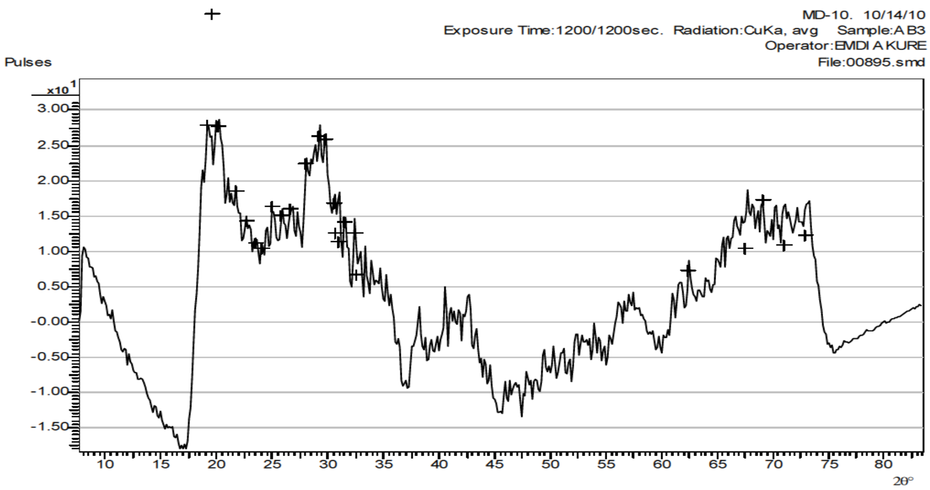

Fig 11: XRD diffractogram for as deposited Cr_2O_3 films annealed at 473K

The film annealed at 673K given by fig. 12, shows peak at 2θ = 65.20°; which corresponds to diffraction line produced by (300) plane; this is in agreement with similar films grown by Wang et al. op cit and Schneider et al. [37].

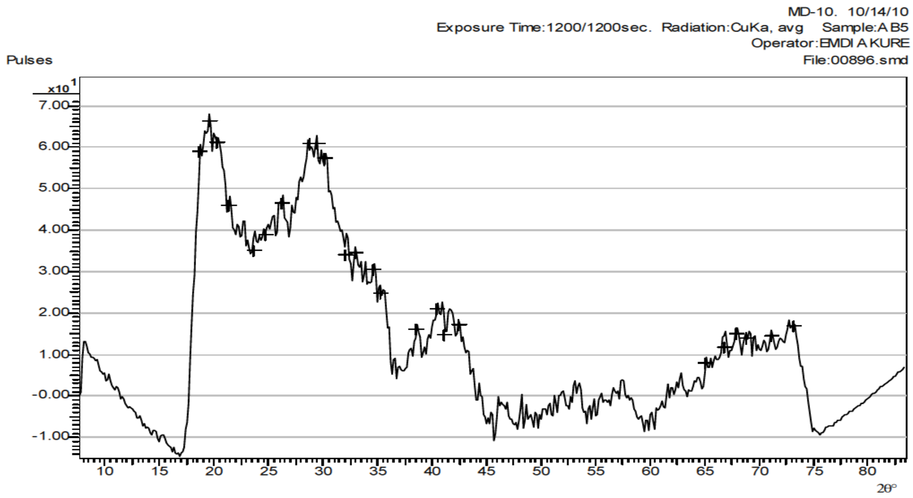

Fig 12: XRD diffractogram for as deposited Cr_2O_3 films annealed at 673K

3.2 Determination of Film Size

Using the Scherer's formula given by equation (5) [38]

$$D = \frac{0.9\lambda}{\beta \cos\theta}, \quad (5)$$

where λ is wavelength of the x-ray, β is full width at half maximum (FWHM) of the peak with highest intensity and θ is the diffraction angle, the grain sizes were obtained to be of range 16.47nm – 27.96nm for increasing annealing temperature.

4. Conclusion

Nanocrystalline films of Cr_2O_3 with crystallite size range 16.47nm – 27.96nm, were successfully deposited on glass substrates using chemical bath deposition technique. Their moderate transmittance in the VIS, gives them advantage for application as anti-dazzling coatings in car windscreen and rear view mirrors. XRD studies reveal that the Cr_2O_3 films have a preferred orientation in the (119) plane. For films annealed at 473K and 673K, the diffraction at 2θ angle of 72.92^{o}C and 65.20^{o}C respectively, were assigned to the diffraction line produced by (1010) and (300) planes. The values of band gap energy exhibited by the films are in the range required for the application of the film as window layer in solar cell fabrication. The low band gap energies of the films also make them suitable for use as absorber material.

References

[1] T Ivanova, K Gesheva, A Cziraki, A Szekeres and E Vlaikova, Journal of Physics: Conference Series **113**, 012030 (2008).
[2] N Popovici, M L Parampes, R C Da Silva, O Monnereau, P M Sousa, A J Silvestre, O Conde Appl. Phys. A **79,** 1409 (2004)
[3] V.M. Bermudez, W.J. DeSisto, J. Vac. Sci. Technol. A **19**, 576 (2001).
[4] A.S. Cao, M.F. Doerner, V.J. Novotny, J. Appl. Phys. 66 (1989) 5315.
[5] V. Teixeira, E. Sousa, M.F. Costa, C. Nunes, L. Rosa, M.J. Carvalho, M. Collares-Pereira, E. Roman, J. Gago, Thin Solid Films **392**, 320 (2001).
[6] Y. Ogino, S. Nakajima, J. Catal. **9**, 251 (1967).
[7] J. Yoo, E.D. Wachsman, Sensor. Actuat. B. **123**, 915 (2007).

[8] J. Hu, H. Li, X. Huang, Electrochem. Sold-State Lett. **8**, A66 (2005).
[9] E. Povoden, A.N. Grundy, L.J. Gauckler, J. Phase Equilib. Diff. **27**, 353 (2006).
[10] F.D. Lai, C.Y. Huang, C.M. Chang, L.A. Wang, W.C Cheng, Microelecton. Eng. **67-68**, 17 (2003)
[11] A. Azens, G. Vaivars, L. Kullman, C.G. Granqvist, Electrochim. Acta **44**, 3059 (1999).
[12] J.D. Kruschwitz, W.T. Pawlewicz, Appl. Opt. **36**, 2157 (1997).
[13] J.C. Fan, S.A. Spura, Appl. Phys. Lett. **30**, 511 (1977).
[14] C.G. Garnqvist, Appl. Phys. A Matr. **52**, 83 (1991).
[15] T. Maruyama, H. Akagi, J. Electrochem. Soc. **143**, 1955 (1996)
[16] R.S. Boorse, J.M. Burlitch, Chem. Mater. **6**, 1509 (1994).
[17] F. Barradas-Olmos, J.R. Vargas-Garcia, J.J. Cruz-Rivera, Mater. Sci. Forum **386**, 353 (2002).
[18] F.K. Perkins, C. Hwang, M. Onellion, Y.G. Kim, P.A. Dowben, Thin Solid Films **198**, 317 (1991)
[19] J. Wang, A. Gupta, T.M. Klein, Thin Solid Films **516**, 7366 (2008).
[20] G. Gheorghies, L. Gheorghies, J. Optoelectron. Adv. Mater. **3**, 107 (2001).
[21] S. Noguchi, M. Mizuhashi, Thin Solid Films **77**, 99 (1981).
[22] X. Pang, K. Gao, F. Luo, H. Yang, L. Qiao, Y. Wang, A.A. Volinsky, Thin Solid Films **516**, 4685 (2008).
[23] P. Borisov, A. Hochstral, V.V. Shvartsman, W. Kleemann, P.M. Hauck, Integr. Ferroelectr. **99**, 69 (2008).
[24] H. Mändar, T. Uustare, J. Aarik, A. Tarre, A. Rosental, Thin Solid Films **515**, 4570 (2007).
[25] R.N. Goyal, D. Kaur, and A.K. Pandey, Materials Chemistry and Physics **116,** 638 (2009).
[26] M. Julkarnain, J. Hossain, K.S. Sharif, and K.A. Khan, Canadian Journal on Chemical Engineering & Technology **3(4)**, 81 (2012).
[27] F. I. Ezema, A.B.C Ekwealor and R.U. Osuji, Superficies y Vacío **21**(1), 6 (2008).
[28] F.I. Ezema, S.C. Ezugwu, P.U. Asogwa, A.B.C. Ekwealor, Journal of Ovonic Research, **5**(5), 145 (2009).
[29] P.E.Agbo, M.N. Nanbuchi, D.U. Onah, Journal of Ovonic Research **7**(2)**,** 29 (2011).
[30] M.F. Al-Kuhaili, S.M.A. Durrani, Optical Materials **29,** 709 (2007).
[31] H.B. Lee, Y.M. Yoo, Y.H. Han, Scripta Mater**. 55,** 1127 (2006).
[32] S.F. Oboudi, S.S. Chiad and N.F. Habubi, Baghdad Science Journal **8(2),** 165 (2011).
[33] M.M. Wakkad, E.Kh. Shokr and S.H. Mohamed, J. of Non-Crystalline Solids, **265**(1-2), 157 (2000).
[34] F.I. Ezema, P.U. Asogwa, A.B.C. Ekwealor, P.E. Ugwuoke and R.U. Osuji, Journal of University of Chemical Technology and Metallurgy, **42(**2), 217 (2007).
[35] F.I. Ezema, S.C. Ezugwu, R.U. Osuji, P.U. Asogwa, B.A. Ezekoye, A.B.C. Ekwealor, M.P. Ogbu, Journal of Non-Oxide Glasses **1(**1), 45 (2010).
[36] D.Y. Wang J.H. Lin, W.Y. Ho, Thin Solid Films **332**, 295 (1998).
[37] Schneider, J.M., Sproul, W.D., Sellers, J. and Matthews, A., In: Soc. Of Vac. Coaters, 40th Annual Technical Conference Proceedings (Society of Vacuum Coaters, 1997), 301.
[38] V. Elena, et al, Thin Solid Films. **365**, 12 (2000).